

## Influence of a macroscopic circuit on polarons in a *p-n* tunnel junction

W. H. Richardson

*Ginton Laboratory MC4085, Department of Applied Physics, Stanford University, Stanford, California 94305-4085*

(Received 28 January 1999)

The tunneling current versus voltage of a degenerate *p-n* junction at milliKelvin temperatures, was observed to be linear or nonlinear depending on the impedance of the external circuit. Unbinding of polarons is the ascribed source of the thresholdlike feature in the conductance. A quantum description of the entire system included coupling of the electrons to two different sets of bosonic particles. The total dielectric function included a contribution due to the circuit, and the resulting spectral function implied damping of the polaron mode. [S0163-1829(99)00819-X]

Investigations of the current-voltage characteristics of tunnel junctions, at low bias voltages, has perennially yielded information about the elementary excitation of the medium, and more generally about the nature of conductors. It is now well accepted that the activation of quasiparticles, such as phonons and polarons, can modify the electrical characteristics of semiconductor tunnel junctions<sup>1-6</sup> and Schottky barriers.<sup>7,8</sup> In general the quanta of energy associated with the creation or destruction of quasiparticles leads to threshold-like features in the I-V of tunnel junctions. The effects of phonons are readily apparent in junctions formed from indirect-bandgap semiconductor material, because in such junctions the generation of phonons is an essential constituent of the tunneling process. Aside from phonon-assisted tunneling, other aspects of electron-phonon coupling can affect tunneling. Formation of polarons can lead to the inhibition of tunneling at low-junction voltages; that is because, if an electron is in a polaron bound state, then the junction voltage must be larger than the threshold associated with the polaron binding energy ( $V > \hbar\omega_g/e$ ) in order to obtain a free electron for tunneling. This direct connection between the tunneling current, polaronic state, and the junction voltage permits exploration of the influence of the external circuit on the polaron. Now, it was recently recognized that due to the Coulomb blockade effect an external circuit can influence the tunneling current in a mesoscopic junction.<sup>9,10</sup> We have observed that the tunneling current—at low-junction voltages—of a macroscopic degenerate *p-n* junction, can be linear or nonlinear depending on the external circuit. At the low temperatures employed in the experiments, the threshold features in the conductance appear to be due to the unbinding of polarons. Our observation reveals that the properties of a quasiparticle can be modified by the macroscopic circuit in which the particle is embedded. In the following discourse, the experimental evidence and supporting theoretical formalism for this new phenomena are presented.

A theory that describes the effects of an external circuit on tunneling in degenerate *p-n* junctions has been developed.<sup>11,12</sup> A simplified representation of the system under consideration is shown in Fig. 1(a). Polarons near the junction are taken into account by including coupling of the electrons to another set of bosonic particles. The computational procedure is similar to that presented in Ref. 11. Hence, only an outline of the derivation of the additional

term will be presented. We started from the additional term in the Hamiltonian that describes tunneling in the presence of bosonic particles:  $H_{IT} = \sum_{k,q,g} [\Lambda_{kqg} c_k^\dagger c_q e^{i\varphi} (b_g + b_g^\dagger) + \text{H.c.}]$ . Here  $\Lambda_{kqg}$  is a coupling constant,  $g$  the Boson wave vector,  $k, q$  are wave vectors for electrons on the *p* and *n* sides of the junction,  $c_q$  the electron annihilation operator, and  $b_g$  the boson annihilation operator. The displacement operator  $e^{i\varphi}$  couples the evolution of the continuous charge distribution (due to the external circuit) to the discrete change of the charge on the junction. Linear response yields an expression for the indirect tunneling current in terms of the Green's function:  $I_i(V, T) = 2e\hbar^{-2} \text{Im}[G^R(\omega \rightarrow -eV)]$ . The transform of that retarded Green's function was evaluated using the Matsubara technique. The Matsubara-Green's function associated with  $G^R$  was found to be  $\mathcal{L}_i(\tau) = 2G_{ec}(\tau) \sum_{k,q,g} |\Lambda_{k,q,g}|^2 G(k, -\tau) G(q, \tau) D(g, \tau)$ , where the Matsubara-Green's function for the noninteracting subsystems are  $G(k, \tau)$  for electrons on the *p* side,  $G_{ec}(\tau)$  for the external circuit, and  $D(g, \tau)$  for the boson field. Series expansion of the Matsubara-Green's function, and with  $G(q, i\omega_q) = \int_0^\beta d\tau G(q, \tau) e^{i\omega_q\tau}$ , then taking the transform of  $\mathcal{L}(\tau)$ , yields  $\mathcal{L}(i\omega_n)$ . The resulting sum over the Bosonic and Fermionic frequencies were evaluated using the Leh-

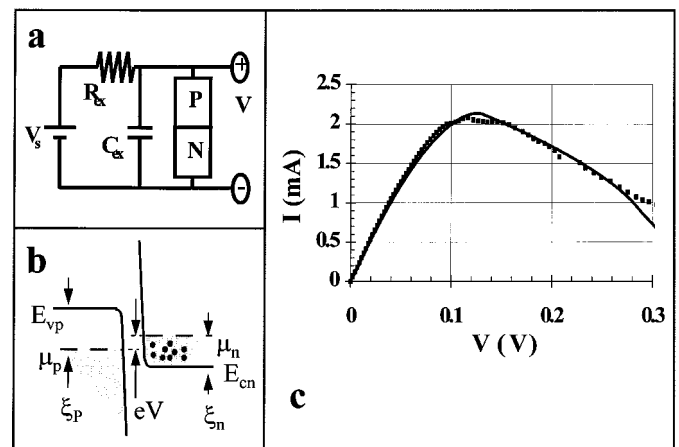


FIG. 1. A simplified schematic of the circuit is shown in (a). In (b) is displayed a diagram of the energy bands for the energy range of interest. (c) The measured current-voltage characteristics (dots), and the theoretical estimate (solid line) of a macroscopic junction, when the junction was connected to a low-impedance source and over a wide range of applied voltage.

mann representation and analytic continuation ( $i\omega_n \Rightarrow -eV + i\delta$ ) yields

$$\begin{aligned}
I_i(V, T) = & \frac{e}{\hbar^2 \pi^3} \sum_{k, q, g} \int_{-\infty}^{\infty} \int_{-\infty}^{\infty} \int_{-\infty}^{\infty} dy dz' dx' \\
& \times \text{Im} G^R(k, y) \text{Im} G^R(q, z') A_{\text{ec}}(p, y - eV - z' - x') \\
& \times \{ |\wedge_{k, q, g}^c|^2 A_c(g, x') + |\wedge_{k, q, g}^b|^2 B(g, x') \} \\
& \times [n_B(y - eV - z' - x') + n_F(-z')] \\
& \times [n_F(y) - n_F(y - eV - x')] \\
& \times [n_B(eV + x') - n_B(x')]. \quad (1)
\end{aligned}$$

Here  $A_{\text{ec}}$  is the spectral function of the external circuit in equilibrium, and  $A_c(g, x')$  the spectral function of phonons that contribute to indirect tunneling;  $n_B$  is the Bose occupation factor, and  $n_F$  the Fermi occupation factor; the equilibrium Green's functions follow from  $G^R(s, \omega) = G(s, i\omega_n \rightarrow \omega + i\delta)$ . The spectral function of the quasibosonic particle that binds with the electron to form a polaron is given by  $B(g, \omega) = -2 \text{Im} D^R(g, \omega)$ . Our approach to treating polaron formation is akin to the normal-mode theory of quantum optics. Effects due to polarons could have been included in the Green's function  $G^R(k, y)$ . The usual procedure is to calculate the self energy in the random-phase approximation with dielectric screening.<sup>13</sup> In the present approach, a bosonic particle of energy  $\hbar\omega_g = \alpha_c \hbar\omega_{\text{LO}}$  is associated with polaron formation, and the Green's functions are those for independent electrons. Factors  $|\wedge_{k, q, g}^c|^2$ , and  $|\wedge_{k, q, g}^b|^2$  are coupling constants for, respectively, indirect tunneling via phonons, and tunneling from polaron states.

The current proportional to  $B(g, \omega)$  is significant. In this system with many interactions, the interaction between the circuit and the coupled electron-phonon system is formulated starting from the total dielectric function  $\varepsilon(g, \omega)$ , and the polarization  $P$ .<sup>13</sup> Here the dressed Green's function is taken as

$$D^R(g, \omega) = \frac{2\omega_g}{\omega^2 - \omega_g^2 - 2\omega_g [M_g^2 P / \varepsilon(g, \omega)]}. \quad (2)$$

In analogy with the case of phonons in metals, we use  $\varepsilon(g, i\omega) = 1 - \nu_g P(g, i\omega) / \varepsilon_m$ . Here  $\varepsilon_m$  is the background or medium dielectric constant,  $\nu_g$  is the unscreened electron-electron interaction, and the coupling constant is given by  $2M_g^2 = \nu_g \omega_g / \varepsilon_m$ . The dielectric function for the entire circuit without polarons is taken as:  $\varepsilon(\omega) = 1 + i\sigma / (\omega\varepsilon_0)$ , from which it follows that  $\varepsilon(\omega) = i\omega R_{\text{es}} C_{\text{es}} / (1 + i\omega R_{\text{es}} C_{\text{es}})$ . Here  $R_{\text{es}}$  is the effective resistance, and  $C_{\text{es}}$  the total effective series capacitance of the circuit in which the polaron will be

embedded. In the case of weak damping we obtain  $B^\pm(g, \omega) \approx \pm \omega_r / (\omega \mp \omega_g)^2 + (\omega_r/2)^2$ , where the spectral function at positive frequencies  $B(g, \omega > 0) \equiv B^+(g, \omega)$ , and similarly  $B(g, \omega < 0) \equiv B^-(g, \omega)$ , with  $\omega_r = 1/(R_{\text{es}} C_{\text{es}})$ . The fact that the spectral function of the quasiparticle proved to be a Lorentzian is the basis for the statement that the external circuit damps the polaron mode. The transition to strong damping is obtained by taking the fraction of electrons in the polaron bound state as:  $\gamma_{\text{pl}} = \int_0^{\xi_p} d\omega B(g, \omega) / (2\pi) \approx [\arctan(\xi_p / \gamma_e) + \arctan(\omega_g / \gamma_e)] / \pi$ .

In the limit of ultralow temperatures, the current can be written in terms of elementary integrals. Some of those integrals must be evaluated numerically. The experimental parameters satisfy the following inequality:  $E_c \leq \xi_p \leq \xi_n + E_c$ . Over that range of parameters the current due to direct tunneling of free electrons (electrons not bound in equilibrium) is given by<sup>12</sup>

$$I_d(V) = A_d \begin{cases} 0, & 0 \leq eV \leq E_c \\ (1 - \gamma_{\text{pl}}/2) K(\xi_n - eV + E_c, \xi_n), & E_c \leq eV \leq \xi_p. \end{cases}$$

Here  $K(\mathcal{E}_1, \mathcal{E}_2)$  denotes the integral over the density of states:  $K(\mathcal{E}_1, \mathcal{E}_2) \equiv \int_{\mathcal{E}_1}^{\mathcal{E}_2} R(\mathcal{E}) d\mathcal{E}$ , with  $R(\mathcal{E}) = (\mathcal{E} - E_{\text{cn}})^{1/2} (E_{\text{vp}} - \mathcal{E})^{1/2}$ .

The current due to indirect tunneling via phonons was evaluated starting from the term [in Eq. (1)] proportional to  $|\wedge_{k, q, g}^c|^2 A_c(g, x')$ . Summation over the phonon wave vector yields the current that is proportional to the phonon density of states  $[\rho_{\text{ph}}(x')]$ :

$$\begin{aligned}
I_{\text{ic}}(V) = & A_i \int_{E_{\text{cm}}}^{E_{\text{vp}}} d\mathcal{E} \int_0^{eV} dx' \frac{\rho_{\text{ph}}(x')}{x'} \\
& \times R(\mathcal{E}) f(\mathcal{E}) f(-\mathcal{E} - eV + x' + E_c). \quad (3)
\end{aligned}$$

The formulation of a term similar to Eq. (3) represented the zenith of application of the Matsubara-Green's function technique to tunneling in semiconductor junctions in the late 1960's.<sup>5</sup> It was shown that that term can describe "certain types" of zero-bias anomalies observed in metal-semiconductor and semiconductor  $p$ - $n$  junctions. More specifically, the anomalies were attributed to the excitation of TA phonons, and the minima in the conductance occurred at bias voltages around  $\hbar\omega_{\text{TA}}/q$ . Our addition to this specific mechanism of inelastic tunneling is not as profound: we included effects due to the Coulomb blockade and density of states. In future mesoscopic  $p$ - $n$  junctions this term can be significant. In heavily doped junctions,  $I_{\text{ic}}$  is smaller than  $I_d$ , and it is also smaller than the term proportional to  $|\wedge_{k, q, g}^b|^2 B$ .

Continuing from Eq. (1), the new phenomena is primarily related to the current due to electrons released from the polaron bound state:

$$I_{\text{pl}}(V) = \frac{A_i \alpha_{\text{ig}} \gamma_{\text{pl}}}{2\hbar\omega_g} \int_0^{\Delta\mathcal{E}} d\mathcal{E} \int_0^{\mathcal{E} + eV - E_c - \xi_n} dx' R(\mathcal{E}) B(g, x') \Theta(\mathcal{E} + eV - E_c - \xi_n) f(\mathcal{E} - \xi_n) \Theta(-\mathcal{E} + E_c + \xi_n). \quad (4)$$

And we find that

$$I_{\text{pl}}(V) = \frac{A_i \alpha_{\text{ig}} \gamma_{\text{pl}}}{2 \hbar \omega_{\text{LO}}} \begin{cases} 0, & 0 \leq eV \leq E_c \\ \int_0^{eV - E_c} dx' B(g, x') K(\xi_n - eV + E_c + x', \xi_n), & E_c \leq eV \leq \xi_p. \end{cases}$$

Collecting all the terms gives the total current at small positive voltages and at ultralow temperatures:  $I(V) + I_d + I_c + I_{\text{pl}}$ .

The experimental arrangement was based on the usual four-point-probe technique. Inner probes [Fig. 1(a)] were used to directly measure the junction voltage.<sup>14</sup> An ac source was added in series with the bias whenever an experimental measurement of  $di/dv$  was feasible. The ac source, and associated lockin detection, were removed if extremely accurate measurement at very small source voltages were required. In that case the conductance was obtained by numerical differentiation of the current-voltage measurements. A voltage source within a few millimeters of the junction was obtained by inserting between the bond lead and substrate of the device, a combination of capacitors with a total capacitance of  $C_{\text{ex}} = 0.1 \mu\text{F}$ . In the case of a high-impedance source, the capacitance parallel to the junction were removed, resistors with an equivalent resistance of  $R_{\text{ex}} = 1 \text{ M}\Omega$  were inserted in series, and the device was driven by a current source. The devices were cooled in a dilution refrigerator.

The energy band diagram, of the device under study, is shown in Fig. 1(b). Experimental and theoretical results are most readily connected by the following parameters: the depth of the degeneracy on the  $n$  side  $\xi_n \equiv \mu_n - E_{\text{cn}}$ , and that on the  $p$  side  $\xi_p \equiv E_{\text{vp}} - \mu_p$ . Here  $\mu_n$  and  $\mu_p$  are the Fermi levels on the  $n$  side and  $p$  side, respectively, and  $\Delta\mathcal{E} \equiv E_{\text{vp}} - E_{\text{cn}} = \xi_n + \xi_p - eV$ . The GaAs junctions featured an acceptor concentration of approximately  $2 \times 10^{19} \text{ cm}^{-3}$ , and a donor concentration estimated to be  $\approx 3 \times 10^{19} \text{ cm}^{-3}$ . The intrinsic junction capacitance was  $C_{ij} = 0.25 \text{ pF}$ , and the intrinsic series resistance (at room temperature)  $R_{is} \approx 7 \Omega$ . At 100 mK, the measured tunneling resistance was typically  $36 \Omega$ , peak current  $I_p = 2.1 \text{ mA}$ , peak voltage  $V_p = 120 \text{ mV}$ , and the minimum negative differential resistance  $R_m = -150 \Omega$ . The resistive cutoff frequency  $f_{r0} = 29 \text{ GHz}$  was much less than the self-oscillation frequency  $f_o = 950 \text{ GHz}$ , thereby enabling stable biasing of the device with even a low-external impedance.

The measured current and theoretical estimate over a wide range of voltage, that includes the region of negative differential resistance, are shown in Fig. 1(c). In that measurement, the device was voltage biased and  $T = 0.19 \text{ K}$ . The parameters employed were  $\xi_p = 0.13 \text{ eV}$ ,  $\xi_n = 0.28 \text{ eV}$ , and  $A_d = 5 \times 10^{36}$ . In principle the Fermi level should be obtained from the doping densities and neutrality condition. However, accurate estimates of the carrier concentrations at low temperatures depend on other parameters that are not well known. The values for  $\xi_p$  and  $\xi_n$  were determined from measurements and using the following relationships: the voltage at which the current is a maximum  $V_p \approx (\xi_p + \xi_n)/(3e)$ ; and the threshold for the thermionic diffusion current is given by  $(E_g + \xi_p)/e$ , where  $E_g$  is the energy bandgap. The excellent

fit establishes the parameters not related to polaron formation, and gives us some confidence in the theoretical formalism.

The conductances for a junction driven by a low-impedance source (trace a), and alternately by a high-impedance source (trace b) are shown in Fig. 2. In the case when the junction was voltage biased the temperature was stable at  $T = 135 \text{ mK}$ , and in the other case  $T = 195 \text{ mK}$ . The conductance for a different device that was voltage biased and at  $T = 80 \text{ mK}$  is given by trace (c). The observed threshold in the conductance [trace (b)] is attributed to the presence of polarons in the conduction band on the  $n$  side of the junction. The current increases at energies (eV) larger than the polaron binding energy, because such voltages are large enough to release the electron from a polaron bound state, thereby enabling tunneling of a bare electron. The measured threshold appears at a voltage  $V_{\text{tp}} = 1.2 \text{ mV}$ , which is slightly less than the theoretical threshold ( $\alpha_c \hbar \omega_{\text{LO}}/e = 2.2 \text{ mV}$ ) for polarons in semi-insulating or lightly doped GaAs. Here  $\alpha_c = 0.062$  is the Frolich coupling constant for electrons in the conduction band, and  $\hbar \omega_{\text{LO}} = 36 \text{ meV}$  is the LO phonon energy. In a heavily doped semiconductor, the theoretical threshold is expected to be smaller than  $\alpha_c \hbar \omega_{\text{LO}}/e$  because screening of the electron-phonon interaction tends to reduce the value of  $\alpha_c$ . A similar value for the measured threshold voltage in GaAs was also obtained by Hall.<sup>4</sup> It is unlikely that polarons in the valence band play a role. Because a calculation of the coupling constants from the Frolich formula  $\alpha = e^2(m^*/2\hbar\omega_{\text{LO}})^{1/2}(1/\epsilon_\infty - 1/\xi_o)/\hbar$  yields for the heavy-hole band  $\alpha_{\text{hh}} = 0.198$ , and for the light hole  $\alpha_{\text{lh}} = 0.083$ . The relevant constants for the participation of

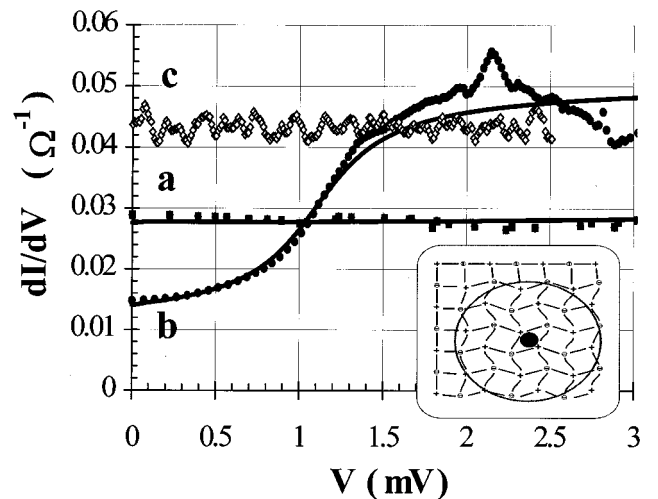


FIG. 2. Comparison of the calculated conductances (solid lines), and those obtained from measurements are shown in the main figure. Trace (a) represents the case when the junction was driven by a low-impedance source, and trace (b) the same device driven by a high-impedance source. Trace (c) is the conductance for another device in a low-impedance environment. A representation of the polaron is shown in the lower inset.

valence-band polarons would be  $\alpha_v = (\alpha_{\text{nh}} + \alpha_{\text{lh}})/2$ , and for cross-band interaction  $\sqrt{\alpha_c \alpha_v}$ . Both constants yield thresholds that are much larger than the measured value. The observed threshold is not associated with the excitation of TA phonons, be it impurity, induced phonons in the transition region or bulk, because in that case the transition would occur around  $\hbar \omega_{\text{TA}} = 8$  mV. The difference in tunneling resistance between the two devices [traces (a) and (c)] is due to the difference in temperature and the slight difference in doping. Contact resistances contribute to the background conductance, and do not affect the value for the measured threshold in  $di/dv$ .

The threshold in the conductance is absent in the case of a low-impedance source because of damping of the polaron. A possible physical picture is as follows. The properties of an electron are affected by the motion of the lattice because of the Coulomb interaction between the electron and ions. Similarly, the presence of an electron leads to polarization of the space around the electron. As an electron moves through the crystal it drags along the associated polarization. A polaron (see the inset of Fig. 2) consists of an electron and the induced polarization (or cloud of virtual-optical phonons). The polaron is said to be large (as is the case in GaAs), if the distortion of the lattice extends over several lattice constants. Tunneling of electrons results in fluctuation of the internal electric field. If the junction is voltage driven, then the process of rapid recharging of the junction (after tunneling of an electron) decouples the electron from the much heavier and slowly moving ions. If the junction is sufficiently isolated, then the gradual recharging does not necessarily lead to decay of the polaron.

The solid lines in Fig. 2 represent the theoretical results. Theoretical estimates were obtained using the previous values for  $\xi_n$  and  $\xi_p$ ,  $\alpha_{ig} = 364$ , and in the high-impedance regime  $\omega_R = 1.0 \times 10^{12} \text{ sec}^{-1}$ , while in the low-impedance case  $\omega_R \geq 3.3 \times 10^{15} \text{ sec}^{-1}$ . In the high-resistance environment, the decay time ( $1/\omega_R$ ) is given by roughly the polaron scattering time since the particle is isolated. The value of  $\hbar \omega_g$  was chosen to match the measured threshold in the conductance, and the coupling constant  $\alpha_{ig}$  practically yields the change in magnitude of the conductance. Clearly the theory, with  $\hbar \omega_g$  and  $\alpha_{ig}$  considered as adjustable parameters, can be used to describe the experimental results. The contribution from  $I_{\text{pl}}$  was obtained by numerical integration;

that current starts around  $eV = \hbar \omega_g$ , and is larger in magnitude than  $I_d$ . In the limit of zero bias, the background conductance is due primarily to the direct tunneling of unbound electrons ( $I_d$ ). Phonon-assisted tunneling current ( $I_{\text{ic}}$ ) is much smaller than  $I_d$ . Outside the voltage range shown in the figure, the calculated conductance is larger than the measured value. That discrepancy is probably due to band-tailing effects.

This observation of the effect of different circuit impedance on tunneling is reminiscent of the Coulomb blockade effect. And it has been suggested that some types of zero-bias anomalies observed in  $p$ - $n$  junctions is due to the Coulomb blockade.<sup>15</sup> However, in our case, it is clear that the observed difference in conductance is not due to Coulomb blockade effects. The measured threshold is much larger than the maximum Coulomb blockade threshold  $V_{\text{ic}} = e/2C_{\text{ij}} = 0.3 \mu\text{V}$ , and in addition  $e^2/(2C_{\text{ij}}k_B T) \approx 0.03$ . Furthermore, the observed threshold cannot be due to a quantum dot (formed from an impurity), because in that type of double-junction system the nonlinearity would still be present when the device is driven by a low-impedance source. The dissimilarity in the physics between the phenomena reported here and Coulomb blockade effects is also clear. The salient feature of Coulomb blockade is that—in the absence of thermal energy—tunneling to a state of higher potential energy is not possible. In the phenomena presented here, the key feature is the modification of the properties of the polaron by the external circuit. The phenomena is in accord with a cherished principle: that the measurement apparatus can disturb the quantity being measured.

In summary, excitement over the measurement of the I-V at low bias voltages is due not only to the fact that it provided information about an elementary excitation, but also because it illustrates the subtle interaction between a quasiparticle and the macroscopic surroundings in which the particle is embedded. A general expression that describes a wide variety of indirect tunneling processes in  $p$ - $n$  tunnel junctions was presented. That expression was evaluated, in the limit of ultralow temperatures, and shown to describe the experimental results.

Partial financial support was provided by the ERATO Quantum Fluctuation Project, and the author thanks Professor Y. Yamamoto.

<sup>1</sup>E. L. Wolf, *Principles of Electron Tunneling Spectroscopy* (Oxford University Press, New York, 1985).

<sup>2</sup>C. B. Duke, in *Solid State Physics*, edited by F. Seitz, D. Turnbull, and H. Ehrenreich (Academic, New York, 1969), Suppl. 10.

<sup>3</sup>R. N. Hall *et al.*, Phys. Rev. Lett. **4**, 456 (1960).

<sup>4</sup>R. N. Hall, in *Proceedings of the International Conference on Semiconductor Physics, Prague, 1960* (Academic, New York, 1960), pp. 193–200.

<sup>5</sup>A. J. Bennett *et al.*, Phys. Rev. **176**, 969 (1968).

<sup>6</sup>J. Bonca and S. A. Trugman, Phys. Rev. Lett. **75**, 2566 (1995).

<sup>7</sup>J. W. Conley and G. D. Mahan, Phys. Rev. **161**, 681 (1967).

<sup>8</sup>D. C. Tsui, Phys. Rev. B **10**, 5088 (1974).

<sup>9</sup>D. V. Averin and K. K. Likharev, in *Mesoscopic Phenomena in Solids*, edited by B. L. Altshuler, P. A. Lee, and R. A. Webb (Elsevier, Amsterdam, 1991).

<sup>10</sup>A. N. Cleland *et al.*, Phys. Rev. Lett. **64**, 1565 (1990); L. J. Geerlings *et al.*, Europhys. Lett. **10**, 79 (1989).

<sup>11</sup>W. H. Richardson, Int. J. Mod. Phys. B **12**, 2513 (1998); Phys. Lett. A **235**, 186 (1997).

<sup>12</sup>W. H. Richardson, Appl. Phys. Lett. **71**, 1113 (1997).

<sup>13</sup>G. D. Mahan, *Many-Particle Physics* (Plenum, New York, 1990).

<sup>14</sup>W. H. Richardson and Y. Yamamoto, Phys. Rev. Lett. **66**, 1963 (1991).

<sup>15</sup>K. Hess *et al.*, Appl. Phys. Lett. **63**, 1408 (1993).